Dalton Transactions

Insertion chemistry of iron(II) boryl complexes

Journal:	*Dalton Transactions*
Manuscript ID	DT-ART-09-2022-002879.R1
Article Type:	Paper
Date Submitted by the Author:	20-Sep-2022
Complete List of Authors:	Narro, Ana; University of Texas at San Antonio, Chemistry Arman, Hadi; UTSA, Chemistry Tonzetich, Zachary; University of Texas at San Antonio, Chemistry

Journal Name

ARTICLE

Insertion chemistry of iron(II) boryl complexes

Ana L. Narro, Hadi D. Arman and Zachary J. Tonzetich*

Received 00th January 20xx,
Accepted 00th January 20xx

DOI: 10.1039/x0xx00000x

www.rsc.org/

Iron(II) boryl complexes of the pyrrole-based pincer ligand, ^{Cy}PNP (^{Cy}PNP = anion of 2,5-bis(dicyclohexylphophinomethyl)pyrrole) have been synthesized and their insertion reactivity interrogated. Compounds of the type, [Fe(BE)(^{Cy}PNP)] (E = pinacholato or catecholato) can be generated by treatment of the precursors, [Fe(OPh)(py)(^{Cy}PNP)] or [FeMe(^{Cy}PNP)] with B_2E_2. The boryl complexes are meta stable, but permit additional reactivity with several unsaturated substrates. Reaction with alkynes, RC≡CR', leads to rapid insertion into the Fe-B bond to generate stable vinyl boronate complexes of the type [Fe(C{R}C{R'}BE)(^{Cy}PNP)] (R, R' = H, Me, Ph, -C≡CPh). Each of the compounds is five-coordinate in the solid state by virtue of coordination of one of the oxygen atoms of the boronate ester. Similar reaction with nitriles, RC≡N (R = Ph, Me), results in facile de-cyanation to produce the correpsonding hydrocarbon complexes, [FeR(^{Cy}PNP)]. In the case of the bulky nitrile 1-AdCN, the insertion intermediate, [Fe(C{Ad}NBpin)(^{Cy}PNP)], has been isolated and structurally characterized. Treatment of the boryl complexes with styrene derivatives results in initial insertion to give an alkylboronate complex follwed by either β-H elimination or protonation to give the products of C-H borylation and hydroboration, respectively.

Introduction

Boryl ligands, BR_2^-, have not featured as prominently in the coordination chemistry of transition elements as other X-type donors.[1-4] Despite this scarcity, metal boryls are known to play prominent roles in various catalytic processes such as hydroboration and C-H functionalization,[5,6] as well as serving as components of chelating ligands.[4,7] The nature of metal-boryl coordination is typically understood to comprise a strong sigma-donation component from the boron lone pair to iron.[8-11] Back-bonding with the boryl unit is generally weak due to poor overlap between the empty *p* orbital on boron and the metal d_π system coupled with competitive π-donation from the boryl substituents.[12,13]

In the area of iron chemistry, work with boryls has traditionally encompassed closed-shell 18-electron compounds of cyclopentadienyl and carbonyl ligands.[14-16] More recently, coordinatively unsaturated and open-shell examples of iron boryls have been proposed as key intermediates in catalytic processes.[17-24] In a few instances, these species have been isolated and subjected to structural characterization (Chart 1).[25-28] The boryl ligands in these complexes are most often generated by reaction of iron precursors with either hydroborane (HBR_2) or diborane (R_2B_2) reagents. Unfortunately, the challenges associated with stabilizing open-shell iron-boryls has resulted in few studies that directly scrutinize the reactivity of the Fe-BR_2 unit directly. Such reactivity is likely of great relevance to catalytic borylation protocols, especially those that make use of binary mixtures of iron salts and simple ligands.[29,30]

Our laboratory recently examined the catalytic mechanism of alkyne hydroboration using an iron pincer system based on the pyrrole-based ligand $^{t\text{Bu}}$PNP displayed in Chart 1.[31] This work built upon methodology first reported by Nishibayashi and coworkers who posited a possible role for four-coordinate iron boryls.[28] In the course of our studies on alkyne hydroboration we observed facile insertion of alkynes into the Fe-B bond. This prompted us to consider the general reactivity of such iron boryls in a system amenable to isolation and characterization. One drawback of the $^{t\text{Bu}}$PNP system, however, is the pronounced bulk of the P^{t}Bu$_2$ donors, which can dramatically attenuate reactivity. In this contribution, we have therefore examined the synthesis and reactivity of iron(II) boryl complexes of the related ^{Cy}PNP ligand containing less sterically encumbering cyclohexyl groups. The boryl compounds have proven to be reactive toward a variety of unsaturated substrates by virtue of facile migratory insertion pathways engaging the Fe-B bond.

Chart 1. Examples of structurally-characterized open-shell iron boryl complexes.

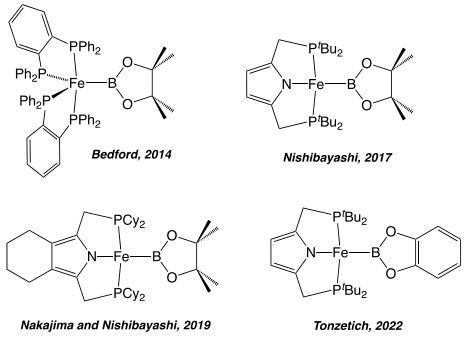

Department of Chemistry, University of Texas at San Antonio (UTSA), San Antonio, TX 78249, USA.
* email: zachary.tonzetich@utsa.edu
Electronic Supplementary Information (ESI) available: NMR spectra, additional thermal ellipsoid drawings. See DOI: 10.1039/x0xx00000x

Results and Discussion

Iron Boryl Synthesis

Prior work with the $^{t\text{Bu}}$PNP ligand established the ability of iron-phenoxide precursors to serve as entry points to stable four-coordinate boryl complexes of iron(II).[31,32] We therefore targeted the previously reported phenoxide complex, [Fe(OPh)(py)($^{\text{Cy}}$PNP)] (**1·py**),[33] as an suitable starting point for synthesis of new metal boryls. Treatment of **1·py** with B_2pin_2 or B_2cat_2 (pin = pinacholato, cat = catecholato) led to smooth formation of purple solutions of the corresponding boryl species (**3**, eq 1) as judged by ^{1}H NMR spectroscopy. Efforts to isolate and fully characterize **3a** or **3b**, however, have been unsuccessful as the complexes are unstable and begin to decompose within a matter of minutes. ^{1}H NMR spectroscopic examination of the reaction mixture evinces broad resonances for the pyridine by-product suggesting that in solution association of the Lewis base is likely occurring in a reversible fashion to either Fe or B.[34] In the solid state we have succeeded in isolating the pyridine adduct of the phenoxy(chatecholato)boron by-product demonstrating that, eventually, the pyridine molecule is sequestered by boron (see Electronic Supplementary Information). Subjecting the reaction mixture to vacuum in order to remove pyridine results in a reversible, rapid colour change from purple to red. If the vacuum is quickly removed, the colour is restored to purple. However, if the solution is allowed to continue under a reduced atmosphere, decomposition is accelerated resulting in a brown mixture of unidentifiable products.

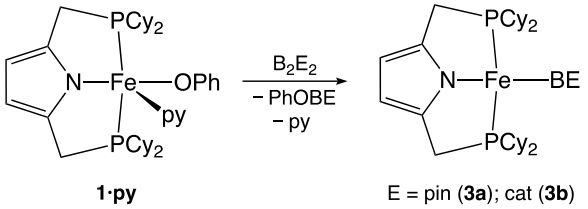

1·py E = pin (**3a**); cat (**3b**) (1)

Scheme 1. Reactions with CO(g) and bipyridine.

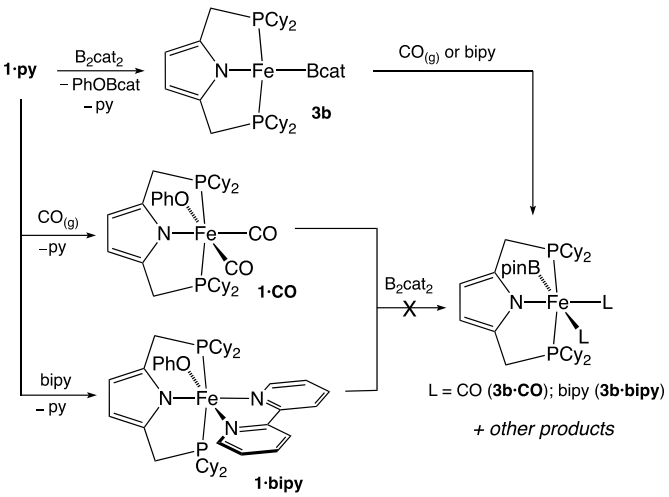

In an attempt to stabilize the putative boryl complexes, we examined addition of both CO and 2,2'-bipyridine to **3b** (Scheme 1). Upon introduction of a CO atmosphere, an immediate colour change from purple to red was observed. ^{1}H NMR analysis showed formation of a single low-spin, diamagnetic complex with C_S symmetry displaying a single ^{31}P NMR shift at δ 82.13. Complementary infrared analysis demonstrated several signals attributable to metal-bound CO groups at 2042, 2018, 1993, 1963, 1934, and 1856 cm^{-1}. We therefore conclude that a mixture of CO-containing complexes is likely present in equilibrium under a CO atmosphere. Of note, CO stretching fundamentals corresponding to the five-coordinate iron(I) dicarbonyl complex, [Fe(CO)$_2$($^{\text{Cy}}$PNP)],[35] are not among the observed peaks suggesting the boryl ligand is still intact (*vide infra*). Nonetheless, the stability of the putative carbonyl adduct, **3b·CO**, is only temporal as NMR spectra recorded one hour after introduction of CO display a mixture of unidentifiable decomposition products. Analogous reactions with **3a** demonstrated similar decomposition behaviour. Accordingly, attempts to isolate either **3a·CO** or **3b·CO** were unsuccessful.

Similar treatment of **3b** with 2,2'-bipyridine (bipy) led to formation of a mixture of products including the previously reported iron hydride species, [FeH(bipy)($^{\text{Cy}}$PNP)],[36] as judged by ^{1}H NMR spectroscopy. Of the new products present, one did show spectral features consistent with a low-spin C_S-symmetric species as expected for a bipyridine adduct of the iron boryl, **3b·bipy** (see ESI). However, this species was found to decompose within a matter of minutes before further analysis could be performed. Reasons for the lack of stability of both **3·CO** and **3·bipy** are speculative, but appear to confirm observations with **3a** that Lewis base association to the metal boryl moiety accelerates decomposition.

In contrast to the chemistry observed upon introduction of CO or bipy to solutions of **3b**, prior coordination of these ligands to **1** resulted in no subsequent reaction with B_2pin_2 or B_2cat_2 even at elevated temperature (Scheme 1). Compounds **1·CO** and **1·bipy** are both octahedral (see ESI for solid-state structures) and lack an open coordination site for reaction with the diboryl reagent. In the case of **1·CO**, its preparation is accompanied by partial loss of the phenoxide moiety and co-crystallization with [Fe(CO)$_2$($^{\text{Cy}}$PNP)].

Given the difficulty in finding a successful synthetic pathway to isolate iron boryl complexes of $^{\text{Cy}}$PNP from **1·py**, we also considered alkyl complexes of $^{\text{Cy}}$PNP as alternative starting points. Indeed, Nishibayashi and coworkers demonstrated successful synthesis of a related boryl complex using such a strategy.[27] We targeted the iron-alkyl, [FeMe($^{\text{Cy}}$PNP)] (**2**) as a precursor reasoning that its reaction with either HBE or B_2E_2 (E = pin or cat) might produce the desired boryl compounds. Treatment of **2** with HBpin resulted in the formation of the bridging-hydride complex, [Fe$_2$(μ-H)$_2$($^{\text{Cy}}$PNP)$_2$],[35] and release of Me-Bpin. By contrast, reaction of **2** with bis(pinacolato)diboron resulted in full conversion to a paramagnetic iron species consistent with **3a** (eq 2). The ^{1}H NMR features of the compound are similar but not identical to those of **3a** prepared from **1·py**. The difference in the NMR features of the

compounds prepared by these two different routes further confirms that the pyridine by-product of the reaction in eq 1 is interacting with **3a** in solution. To test this point more directly, we next added pyridine to a sample of **3a** prepared from **2**. An immediate colour change from green to the expected purple was observed and the ^{1}H NMR spectrum matched that of **3a** prepared from **1·py**. Likewise, addition of CO to pyridine-free samples of **3a** resulted in **3a·CO** as judged by NMR spectroscopy, but the compound was observed to undergo similar rapid decomposition as the material prepared according to Scheme 1. Compound **3a** itself when prepared in the absence of pyridine appears to be significantly more stable in solution. Unfortunately, however, we have still been unable to isolate it or its congener **3b** as a solid compound.

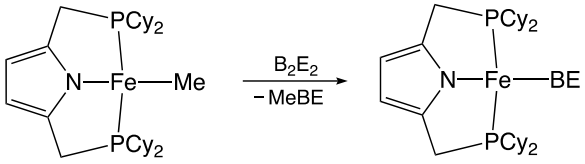

2 E = pin (**3a**); cat (**3b**) (2)

Insertion Chemistry

Despite the challenges in isolating **3a** and **3b**, in situ generation of the compounds has permitted an examination of their reaction chemistry with unsaturated substrates. We began by testing the propensity for alkyne insertion based on the success of similar reactions with the $^{t\text{Bu}}$PNP system.[31] Treatment of **3a** or **3b** prepared from either **1·py** or **2** with 2-butyne resulted in a rapid colour change from purple to bright yellow. NMR spectroscopy confirmed the formation of new *S* = 1 iron complexes in each case consistent with the insertion products **4a,b** displayed in Scheme 2. Structural characterization of **4b** shows the expected new vinyl ligand arising from migratory insertion of the alkyne into the Fe-B bond. In addition, a close contact is present between the iron centre and one of the oxygen atoms of the aryloxyborane unit (Figure 1). Comparing the Fe-O distance in compound **4b** with that of the related vinylboronate compound of $^{t\text{Bu}}$PNP reported previously reveals a contraction of 1.01 Å in the former consistent with coordination of the catecholato oxygen. The presence of this interaction in **4b** is presumably due to the less sterically congested nature of the compound in the vicinity of the metal centre. This interaction must be fluxional in solution, however, as NMR spectra of the compound and all other insertion species described below demonstrate a single set of resonances for equivalent H atoms of the catecholato/pinacolato groups.

Similar insertion behaviour with **3a,b** was observed with the terminal alkyne phenylacetylene (Scheme 2). The new vinylboronate compounds **5a,b** display similar NMR features to **4a,b**, consistent with an intermediate spin iron centre. Crystallographic analysis of both species demonstrated insertion of the phenylacetylene in a 2,1-fashion with the phenyl group bound to the alpha carbon (Figure 1). As in **4b**, both complexes **5a,b** also showed a bonding interaction between the iron centre and one of the boronate oxygens.

Journal Name

ARTICLE

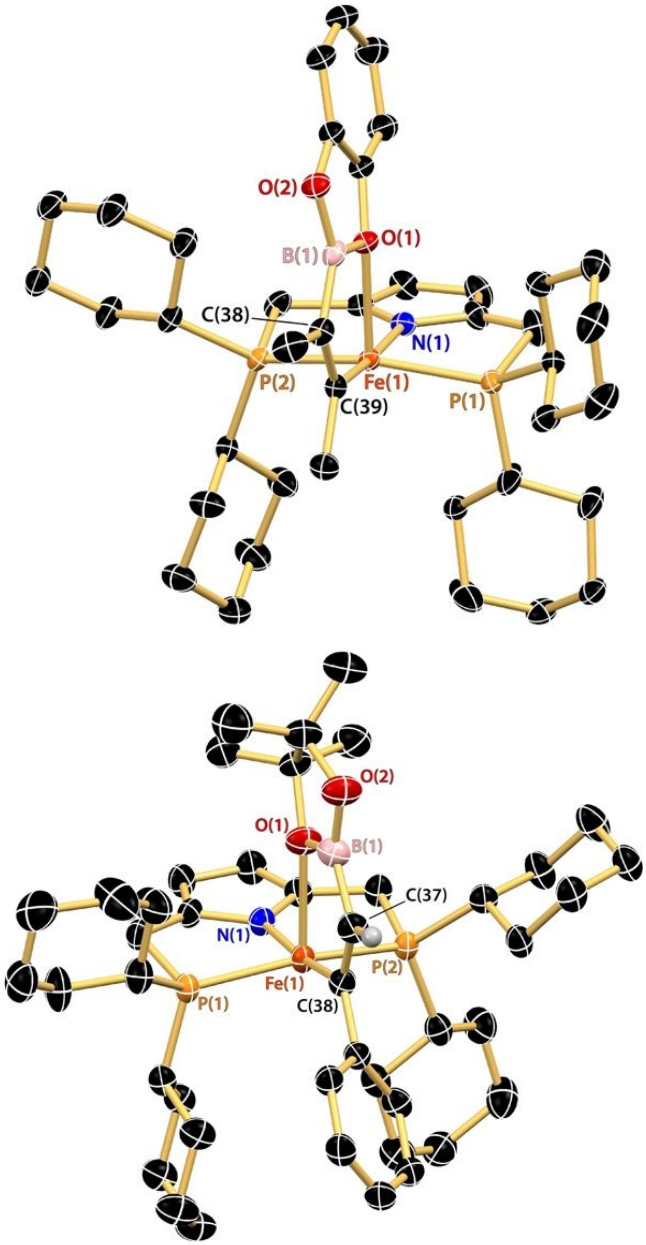

Figure 1. Thermal ellipsoid (50%) drawings of the solid-state structures of **4b** (left) and **5a** (right). Hydrogen atoms omitted for clarity. Selected bond distances (Å) and angles (deg): **4b** Fe(1)-C(39) = 1.9801(18); Fe(1)-O(1) = 2.3389(12); Fe(1)-N(1) = 1.9459(15); Fe(1)-P_{avg} = 2.2760(5); P(1)-Fe(1)-P(2) = 157.06(2); N(1)-Fe(1)-C(39) = 174.74(7); N(1)-Fe(1)-O(1) = 94.44(5); Fe(1)-C(39)-C(38) = 119.81(13); **5a** Fe(1)-C(38) = 1.979(3); Fe(1)-O(1) = 2.3442(6); Fe(1)-N(1) = 1.940(3); Fe(1)-P_{avg} = 2.2868(10); P(1)-Fe(1)-P(2) = 158.26(4); N(1)-Fe(1)-C(39) = 171.45(15); N(1)-Fe(1)-O(1) = 91.46(5); Fe(1)-C(39)-C(40) = 117.8(3).

Scheme 2. Alkyne insertion reactivity of **3a** and **3b**.

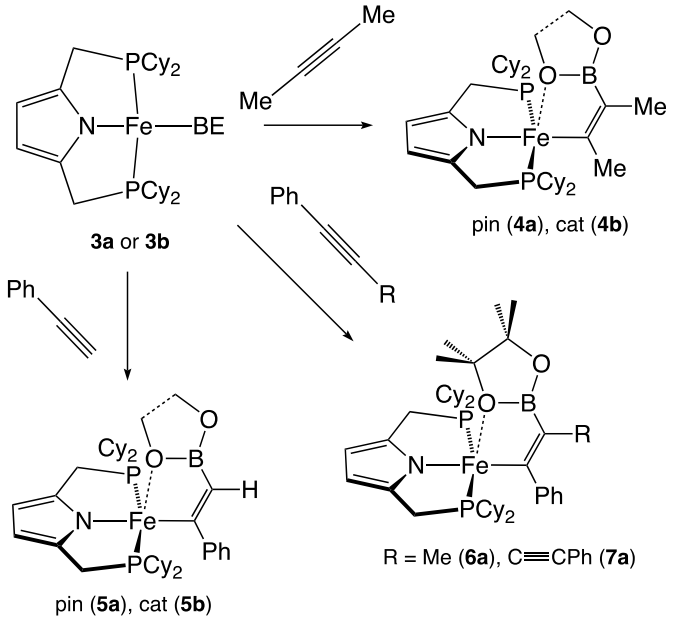

To further probe the regioselectivity of insertion, we also examined the reaction of **3a** with the unsymmetrical alkynes, 1-phenyl-1-propyne and 1,4-diphenylbutadiyne. In both cases, insertion proceeded smoothly to generate the expected vinylboronates (**6a** and **7a**, Scheme 2). Crystallographic analysis of both species confirmed the location of the phenyl group in the α-position akin to insertion reactions with phenylacetylene (see ESI). Therefore, the thermodynamically favoured products of insertion in all cases examined appear to be those where the phenyl substituent is attached to the iron-bound carbon atom. We also attempted to prepare a bimetallic species with 1,4-diphenylbutadiyne whereby the two iron centres are bridged through the original diyne moiety. However, treatment of **3a** with half an equivalent of 1,4-diphenylbutadiyne did not yield the desired complex, either at room temperature or 70 °C, and only resulted in a 50% yield of **7a** as judged by ^{1}H NMR spectroscopy.

With compounds **4**-**7** in hand, we next probed the ability of selected vinylboronate species to undergo further reactivity with hydroborane. Such reactivity would establish a potential role for vinylboronate compounds of ^{Cy}PNPFe as intermediates or resting states in catalytic cycles for hydroboration. Unfortunately, treatment of compounds **4b** and **5b** with HBpin resulted in no reaction at room temperature as judged by ^{1}H NMR spectroscopy. Heating the reaction mixture to 70 °C for 12 h likewise resulted in no significant change in the spectra, although small amounts of a new paramagnetic species were apparent in the case of **4b**. These results contrast those of the related vinylboronate, [Fe(C{Me}C{Me}Bpin)(^{tBu}PNP)], which was found to undergo reaction with HBpin to produce a diborated alkene and [FeH(^{tBu}PNP)].[31] We believe the inability of the ^{Cy}PNP system to engage in comparable chemistry is due to the Fe-O bonding interaction (*vide supra*), which is absent in the ^{tBu}PNP system. Donation of the oxygen lone pairs to iron effectively competes with incoming HBpin shutting down reactivity. This fact paired with the instability of the hydride compound, [FeH(^{Cy}PNP)], likely accounts for our inability to observe productive hydroboration catalysis in the ^{Cy}PNP system.

Moving on from alkynes we turned our attention to insertion reactions of isolobal nitriles. Treatment of in situ-generated **3a** with benzonitrile resulted in an immediate colour change from purple to red followed quickly by the appearance of a dark green solution over several minutes. ^{1}H NMR analysis of the dark green solution evinced formation of the previously reported iron(II) phenyl complex, [FePh(^{Cy}PNP)]. Identical reactions with acetonitrile followed a similar sequence of colour changes leading to formation of the methyl complex, [FeMe(^{Cy}PNP)]. The de-cyanation reactivity of **3a** with nitriles is consistent with a process involving insertion of the C≡N triple bond into the Fe-B unit followed by elimination of CNBpin (Scheme 3).[37] Esteruelas and coworkers have provided evidence for this mechanism in prior work using a pincer ligated Rh(I)-boryl complex.[38] De-cyanation with the rhodium system was significantly slower than observed with iron here, permitting isolation and structural characterization of the nitrile insertion product.

Scheme 3. Reactivity of **3a** with nitriles.

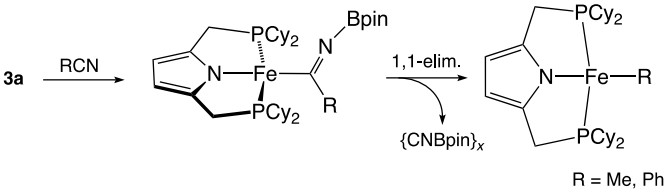

In an attempt to isolate the nitrile insertion product, we considered the very bulky substrate, 1-adamantylnitrile, reasoning that CNBpin extrusion would be slowed by the bulk of the adamantly unit. Reaction with **3a** produced the expected colour change to red, but no subsequent change to green was observed. NMR spectra of the reaction mixture demonstrated formation of a new paramagnetic species with apparent C_S symmetry. Moreover, a singlet resonance for the pinacholato methyl groups was apparent at 3.0 ppm indicating retention of the boryl unit. Crystallographic analysis of material confirmed its identity as the desired insertion product, **8** (eq 3).

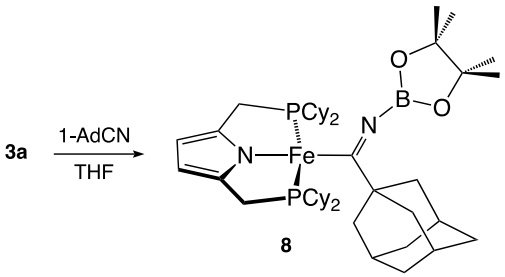

(3)

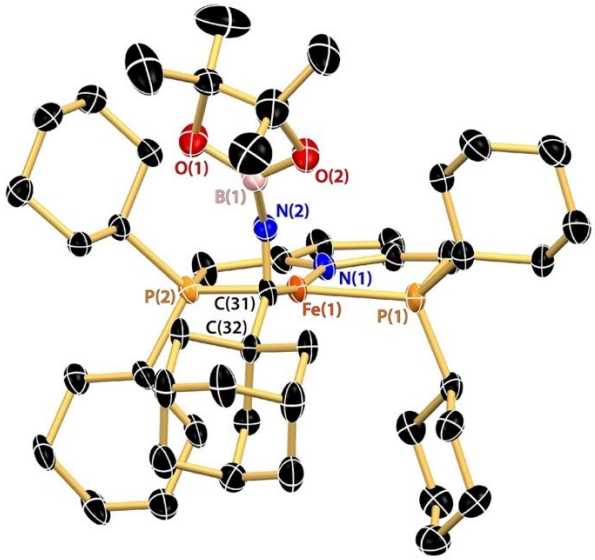

Figure 2. Thermal ellipsoid drawing (50%) of the solid-state structure of **8**. Hydrogen atoms, co-crystallized heptane molecule, and minor components of the disorder omitted for clarity. One of two crystallographically-independent molecules in the unit cell is displayed. Selected bond distances (Å) and angles (deg): Fe(1)-C(31) = 1.929(4); Fe(1)-N(1) = 1.942(3); Fe(1)-P_{avg} = 2.277(1); C(31)-N(2) = 1.264(5); N(2)-B(1) = 1.392(6); P(1)-Fe(1)-P(2) = 162.95(5); N(1)-Fe(1)-C(31) = 169.05(17); C(31)-N(2)-B(1) = 146.5(4).

The solid-state structure of **8** is depicted in Figure 2 and shows the expected molecular configuration for the intermediate along the pathway to nitrile de-cyanation. Unlike **4**-**7**, the boronate oxygen atoms of **8** do not coordinate to the iron centre. The complex is square planar with metal-ligand distances of the inner coordination sphere in line with those of compounds **4**-**7**. The adamantyl group is bound to C_α, consistent with a 2,1-insertion of the nitrile moiety into the Fe-B. Heating solutions of **8** did not result in formation of [FeAd(^{Cy}PNP)] and CNBpin, likely as a result of the combined bulk of the adamantyl group and the Bpin unit. We note that Wilkinson has observed analogous 1,1-elimination from the 1-adamantylacyl group of [CpFe(CO)$_2$(C{O}Ad)], although the reaction was reported to be very sluggish in the absence of high temperatures or UV irradiation.[39]

As a final class of substrates, we examined the reactivity of olefins with compound **3a**. Treatment of **3a** with stoichiometric quantities of styrene led to formation of the bimetallic hydride species, [Fe$_2$(μ-H)$_2$(κ_2,μ-^{Cy}PNP)$_2$],[35] as the predominant iron-containing compound as judged by ^{1}H NMR. Identification of the organic by-products was hampered by the myriad of resonances in the olefinic region, so we shifted focus to para-substituted styrenes. Accordingly, reaction of both 4-methoxy and 4-fluorostyrene with **3a** proceeded to give the same iron hydride species along with several new organic products in similar fashion to the parent styrene. In the case of the fluorinated derivative, examination of the ^{19}F NMR spectrum evinced near full consumption of the olefinic starting material with the appearance of several new organic products (see ESI). These new species were identified as the *E*-vinylboronate ester (ca. 67%), the *gem*-vinylboronate ester (ca. 2%), the linear alkylboroante ester (ca. 9%) and the branched alkylboronate ester (ca. 22%) based on comparison of the ^{19}F chemical shift with literature values (Scheme 4).[40-44]

Scheme 4. Reactivity of **3a** with 4-fluorostyrene.

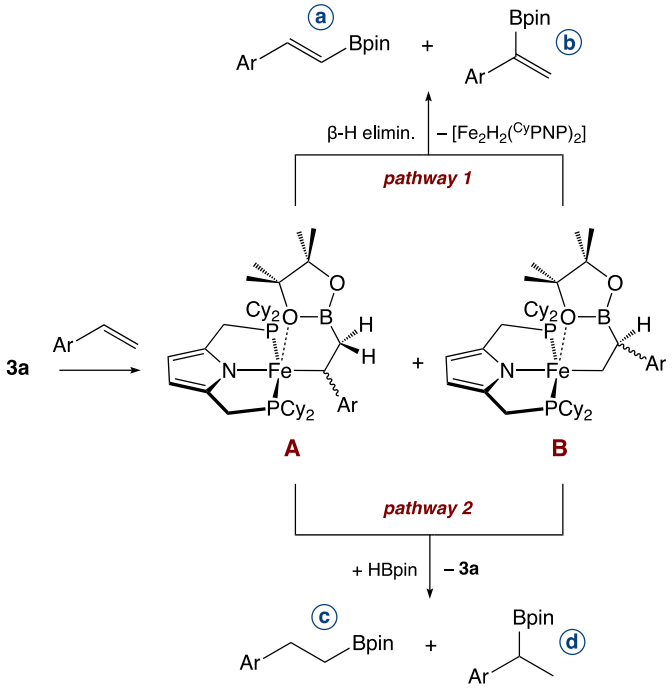

The appearance of the four borylation products is consistent with multiple pathways for the initial insertion products as displayed in Scheme 4.[45] Products (a) and (c) arise from a common intermediate **A**, generated from 2,1-insertion of the styrene into the Fe-B bond. Similarly, products (b) and (d) stem from intermediate **B**, produced by initial 1,2-insertion. Following formation of the alkyboronate intermediates (**A** and **B**), we posit that a competition occurs between β-H elimination (pathway 1) and proton transfer (pathway 2). Pathway 1 is likely favoured for intermediate **A** as there are two β-hydrogen atoms available for elimination. There is also greater steric hinderance about the vicinity of the metal centre, hampering a protonation event, which would be bimolecular. By contrast, the intermediate arising from initial 1,2-insertion has only a single β-hydrogen atom and less steric congestion favouring pathway 2. We can only speculate at this time the origin of the proton source in pathway 2, although it is reasonable to assume that the iron hydride generated by β-H elimination (pathway 1) can further react with B_2pin_2 to produce HBpin.

Preliminary catalytic studies with HBpin and 4-fluorostyrene indicate that **3a** is capable of consuming 20 equiv of styrene in a matter of minutes to produce a distribution of borylated species similar to that obtained in stoichiometric reactions described above. Under catalytic conditions, however, the product distribution changes, with boronates (a) and (d) predominating in a 1 to 7 ratio, respectively. The preference for hydroboration over C-H borylation in catalytic reactions is likely a consequence of the greater concentration of HBpin, which is

capable of intercepting alkylboronate intermediates such as **B** before β-H elimination can occur.

Conclusions

In this study we have examined the synthesis and reactivity of iron(II) boryl complexes of the dicyclohexylphosphine-substituted pincer ligand, ^{Cy}PNP. Synthesis of iron Bpin and Bcat derivatives was accomplished through facile metathetical reactivity between diborane and either phenoxide or methyl precursors. Unlike compounds of the related *tert*-butylphopshine analog, ^{tBu}PNP, boryl complexes of ^{Cy}PNP proved more challenging to isolate but still demonstrated spectroscopic features consistent with four-coordinate intermediate spin (S = 1) species. The reduced steric encumbrance about the metal centre with ^{Cy}PNP likely accounts for the greater reactivity with Lewis bases, which accelerates decomposition pathways. Despite this instability, in situ generation of [Fe(BE)(^{Cy}PNP)] permitted reactivity studies with a variety of unsaturated substrates including alkynes, nitriles, and alkenes. In each case, the initial products of these reactions were consistent with migratory insertion into the Fe-B bond. In many instances, these insertion products were further stabilized by intramolecular coordination of the boronate oxygen atom, a feature not present in compounds of ^{tBu}PNP. Subsequent transformations of the boryl insertion products led to products of de-cyanation, hydroboration, and C-H borylation. These findings therefore highlight multiple diverse roles for Fe-B insertion in a variety of functionalization protocols involving boron.

Experimental

General Comments. Manipulations of air- and moisture-sensitive materials were performed under an atmosphere of purified nitrogen gas using standard Schlenk techniques or in a Vacuum Atmospheres glovebox. Tetrahydrofuran, diethyl ether, pentane, and toluene were purified by sparging with argon and passing through two columns packed with 4 Å molecular sieves (all solvents) and alumina (THF and ether). Heptane, toluene-d_8, and benzene-d_6 were dried over sodium ketyl and vacuum-distilled prior to use. ^{1}H NMR spectra were recorded in benzene-d_6 or toluene-d_8 on a Bruker spectrometers operating at 300 MHz (^{1}H) and referenced to the residual protium resonance of the solvent. FT-IR spectra were recorded with a ThermoNicolet iS 10 spectrophotometer in benzene-d_6 or toluene-d_8 solution using an airtight liquid transmission cell (Specac OMNI) with KBr windows. Elemental analyses were performed by the CENTC facility at the University of Rochester. In each case, recrystallized material was used for the combustion analysis.

Materials. [Fe(py)(OPh)(^{Cy}PNP)] (**1·py**) and [FeMe(^{Cy}PNP)] (**2**) were prepared according to published procedures or slight modifications thereof.[35] Carbon monoxide gas was obtained from Airgas and delivered to reaction mixtures via a syringe needle/septum. All other reagents were procured from commercial suppliers and used as received.

Crystallography. Crystals suitable for X-ray diffraction were mounted, using Paratone oil, onto a nylon loop. Data were collected at 100.0(1) K using a XtaLAB Synergy/ Dualflex, HyPix fitted with CuK_α radiation (λ = 1.54184 Å). Data collection and unit cell refinement were performed using the CrysAlisPro software.[46] Data processing and absorption correction were accomplished with CrysAlisPro and SCALE3 ABSPACK,[47] respectively. The structure, using Olex2,[48] was solved with the ShelXT structure solution program using direct methods and refined (on F^2) with the ShelXL refinement package using full-matrix, least squares techniques.[49,50] All non-hydrogen atoms were refined with anisotropic displacement parameters. All hydrogen atom positions were determined by geometry and refined by a riding model.

[Fe(CO)$_2$(OPh)(^{Cy}PNP)], 1·CO. This compound was prepared in situ by treatment of **1·py** with one atm of CO(g) in benzene-d_6. Upon addition of CO, the solution changed colour from light orange to olive green. The solution was subjected to NMR analysis to confirm formation of **1·CO** and used for subsequent reaction with B_2Pin_2. Vapor diffusion of pentane into benzene solutions containing **1·py** and CO(g) afforded a mixture of orange and green crystals suitable for X-ray diffraction. The green crystals are the previously reported iron(I) compound, [Fe(CO)$_2$(^{Cy}PNP)], and the orange crystals are **1·CO**. NMR (C_6D_6): ^{1}H δ 7.31 (t, 2 m-Ar*H*), 6.88 (d, 2 *o*-ArH), 6.70 (t, 1 *p*-Ar*H*), 6.60 (s, 2 pyr-C*H*), 3.31 (dt, 2 CH_2P), 3.15 (dt, 2 CH_2P), 2.38 (m, 2 Cy) 1.98 (m, 4 Cy), 1.95 (app d, 2 Cy), 1.90 (app d, 2 Cy), 1.77 (app d, 2 Cy), 1.67 (app t, 2 Cy), 1.61 (m, 6 Cy), 1.53 (app d, 2 Cy), 1.46 (m, 6 Cy), 1.35 (app d, 2 Cy), 1.24 (m, 2 Cy), 1.12 (m, 2 Cy), 1.02 (m, 4 Cy), 0.90 (m, 2 Cy), 0.83 (m, 2 Cy); ^{31}P δ 84.09. IR (C_6D_6): cm^{-1} 2002 (ν_{CO}), 1943 (ν_{CO}).

[Fe(bipy)(OPh)(^{Cy}PNP)], 1·bipy. A scintillation vial was charged with 0.128 g (0.18 mmol) of **1·py** and 5 mL of Et_2O. To the solution was added 0.031 g of bipyridine (0.020 mmol) as a solid in one portion. Upon addition of bipyridine, the solution colour rapidly turned to a dark forest green. The mixture was allowed to stir for 5 minutes at room temperature and then the vial was placed in the freezer at −30 °C. After two days at −30 °C, crystalline solids had formed in the vial and were isolated by filtration to afford 0.122 g (86 %) of a green solid. Crystals suitable for X-ray diffraction were grown by similar cooling of a saturated Et_2O solution at −30 °C. NMR (C_6D_6): ^{1}H δ 32.86 (br), 31.14 (br), 22.57 (br), 11.13 (br), -23.54 (br). Anal. Calcd for $C_{46}H_{63}FeN_3OP_2$: C, 69.78; H, 8.02; N, 5.31. Found: C, 69.53; H, 8.36; N, 5.14.

[Fe(Bpin)(^{Cy}PNP)], 3a. Solutions of **3a** were generated in situ by reaction of **1·py** or **2** with an equimolar amount of B_2pin_2. ^{1}H NMR spectroscopic features for **3a** produced from each precursor are as follows: From **1·py**: (C_6D_6) δ 7.6 (br s, 12 Bpin), 0.67 (br s, 4H), -1.41 (s, 4H), -1.94 (s, 4H), -2.14 (s, 4H), -4.5 (br s, 4H), -5.4 (br s, 4H), -9.4 (br s, 4H), -10.4 (br s, 4H), -12.1 (br s, 4H), -44.4 (v br s, 4H); from **2**: (C_7D_8) δ 12.4 (br s, 12 Bpin), 0.74 (m, 4H), 0.08 (s, 4H), -4.32 (s, 4H), -4.7 (br s, 8H), -10.8 (br s, 8H), -11.8 (br s, 2 pyr-C*H*), -14.9 (br s, 4H), -18.7 (br s, 4H), -19.5 (br s, 4H), -22.6 (br s, 4H), -54.1 (br s, 4H).

[Fe(Bcat)(^{Cy}PNP)], 3b. This compound was generated in situ by reaction of **1·py** with an equimolar amount of B_2cat_2. NMR (C_6D_6): ^{1}H δ 0.51 (s, 4H), -0.7 (br s, 4H), -3.6 (br s, 4H), -4.9 (br, 8H), -10.6 (br s, 4H), -12.9 (br, 4H), -14.8 (v br s, 2H), -20.1 (br, 8H), -59.2 (br s, 4H).

[Fe(C{Me}C{Me}Bpin)(^{Cy}PNP)], 4a. This compound was prepared on small scale for spectroscopic analysis by addition of an equimolar amount of 2-butyne to **3a** as prepared above. NMR (C_6D_6): ^{1}H δ 55.96 (br s, 3 Me), 5.76 (br s, 2H), 0.80 (app d, 2H), 0.68 (app m, 2H), 1.09 (app d, 2H), -1.27 (s, 12 B*pin*), -1.80 (s, 2H), -2.21 (s, 2H), -2.58 (s, 2H), -2.9 (br s, 2H), -3.31 (s, 2H), -3.44 (s, 2H), -4.01 (s, 2H), -4.47 (app t, 2H), -5.23 (app d, 2H), -5.74 (br s, 2H), -6.5 (br s, 2H), -7.91 (app d, 2H), -10.88 (br s, 4H), -12.44 (br s, 2H), -12.8 (br s, 2H), -19.5 (br s, 2H), -23.34 (s, 3 Me), -24.82 (s, 2H), -36.01 (br s, 2H), -46.75 (br s, 2H), -48.47 (br s, 2H).

[Fe(C{Me}C{Me}Bcat)(^{Cy}PNP)], 4b. A flask was charged with 0.100 g (0.14 mmol) of **1·py** and 5 mL of THF. While stirring, 0.037 g (0.15 mmol) of B_2cat_2 was added to the solution. The colour changed over the course of a few minutes from light brown to deep purple. After the full colour change took place, 12 μL (0.15 mmol) of 2-butyne was added to the still stirring mixture. The colour rapidly changed to bright yellow and the mixture was allowed to continue stirring overnight. All volatiles were removed in vacuo, and the remaining residue was extracted into toluene and filtered through a Celite pad. The toluene was then removed under reduced pressure and the residue was washed with pentane and collected by filtration to afford 0.071 g (71 %) of yellow solid. Crystals suitable for X-ray diffraction were grown from a saturated heptane solution at −30 °C. NMR (C_6D_6): ^{1}H δ 48.92 (br s, 3 Me), 16.87 (s, 2 cat-C*H*), 5.86 (s, 2 cat-C*H*), 1.63 (app d, 2H), -0.91 (app t, 2H), -1.00 (app d, 2H), -2.10 (app q, 2H), -2.47 (app t, 2H), -2.93 (app q, 2H), -3.09 (app d, 2H), -3.74 (br s, 2H), -4.02 (br s, 2H), -4.11 (app d, 2H), -4.84 (app t, 2H), -5.32 (m, 4H), -6.24 (br s, 2H), -6.81 (app d, 2H), -8.23 (br s, 2H), -8.63 (br s, 2H), -9.63 (br s, 2H), -10.68 (br s, 2H), -16.58 (br s, 2H), -18.7 (br s, 2H), -26.44 (s, 3 Me), -27.31 (s, 2H), -33.22 (br s, 2H), -34.08 (br s, 2H), -72.73 (br s, 2H). Anal. Calcd for $C_{40}H_{60}BFeNO_2P_2$: C, 67.14; H, 8.45; N, 1.96. Found: C, 66.67; H, 8.38: N, 1.77.

[Fe(C{Ph}C{H}Bpin)(^{Cy}PNP)], 5a. A scintillation vial was charged with 0.084 g (0.12 mmol) of **1·py** and 5 mL of THF. While stirring, 0.033 g (0.13 mmol) of B_2pin_2 was added to the solution. After 10 minutes the colour of the reaction mixture changed from light brown to deep purple. After this time, 14 μL (0.13 mmol) of phenylacetylene were added to the still stirring mixture. The colour rapidly changed to vivid red, and the mixture was left stirring for 12 h. All volatiles were removed under vacuum and the remaining residue was extracted into toluene. The mixture was filtered through a pad Celite and the toluene evaporated to dryness. The resulting material was washed with pentane and collected by filtration to afford 0.063 g (69 %) of red powder. Crystals suitable for X-ray diffraction were grown from a saturated heptane solution at −30 °C. ^{1}H NMR (C_6D_6): δ 30.70 (br s, 2H), 14.64 (br t, 1H), 12.09 (d, 2H), 0.30 (app d, 4H), -0.73 (app t, 2H), -1.50 (app d, 2H), -2.05 (s, 12 B*pin*), -2.60 (app d, 2H), -2.82 (br s, 2H), -3.10 (m, 4H), -3.66 (m, 4H), -4.83 (br s, 2H), -5.45 (app t, 2H), -6.29 (br s, 2H), -7.39 (br s, 2H), -7.95 (d, 2H), -8.30 (d, 2H), -8.46 (br s, 2H), -10.74 (br s, 2H), -12.61 (br s, 2H), -13.99 (br s, 2H), -22.83 (br s, 2H), -23.81 (s, 2H), -36.21 (br s, 2H), -40.80 (br s, 2H), -50.92 (br s, 2H), -90.9 (br s, 1H). Anal. Calcd for $C_{44}H_{68}BFeNO_2P_2$: C, 68.49; H, 8.88; N, 1.82. Found: C, 68.77; H, 9.18; N, 1.72.

[Fe(C{Ph}C{H}Bpin)(^{Cy}PNP)], 5b. A flask was charged with 0.100 g (0.14 mmol) of **1·py** and 5 mL of THF. While stirring, 0.037 g (0.15 mmol) of B_2cat_2 was added to the solution. The colour changed over the course of a few minutes from light brown to deep purple. After the full colour change took place 16 μL (0.15 mmol) of phenylacetylene was added to the still stirring mixture. The colour rapidly changed to bright scarlet, and the mixture was allowed to stir for an additional 12 h. All volatiles were removed in vacuo and the remaining residue was extracted into toluene and filtered through a Celite pad. The toluene was then removed under reduced pressure and the residue was washed with pentane and collected by filtration to afford 0.792 g (74 %) of a red solid. Crystals suitable for X-ray diffraction were grown from a saturated heptane solution at −30 °C. NMR (C_7D_8): ^{1}H δ 26.9 (br s, 2H), 15.89 (s, 2 cat-C*H*), 13.07 (br t, 1H), 10.61 (d, 2H), 5.76 (s, 2 cat-C*H*), 1.78 (app d, 2H), -1.30 (app d, 2H), -2.47 (app q, 2H), -2.61 (app q, 2H), -2.81 (app br s, 4H), -4.34 (app d, 2H), -4.47 (app t, 4H), -4.84 (app d, 2H), -5.40 (app q, 4H), -6.19 (br s, 2H), -6.91 (br s, 2H), -7.21 (br s, 2H), -8.12 (br s, 2H), -9.59 (app d, 2H), -10.16 (br s, 2H), -12.29 (br s, 2H), -17.5 (br s, 4H), -26.13 (br s, 2H), -26.87 (s, 2H), -31.29 (br s, 2H), -71.44 (br s, 1 PhCC*H*), -84.48 (br s, 2H). Anal. Calcd for $C_{44}H_{60}BFeNO_2P_2$: C, 69.21; H, 7.92; N, 1.83. Found: C, 68.90; H, 7.87; N, 1.71.

[Fe(C{Ph}C{Me}Bpin)(^{Cy}PNP)], 6a. A flask was charged with 0.094 g (0.13 mmol) of **1·py** and 5 mL of THF. While stirring, 0.036 g (0.14 mmol) of B_2pin_2 were added to the light brown solution. After 10 minutes of stirring the solution changed colour to deep purple and 17 μL (0.14 mmol) of 1-phenyl-1propyne was mixed in. The colour immediately changed to red, and the reaction was allowed to stir for an additional 12 h. All volatiles were removed in vacuo and the remaining residue extracted into toluene and filtered through a pad of Celite. The toluene was evaporated to dryness and the remaining solids were washed with cold pentane and collected by filtration affording 0.083 g (80 %) of red solid. Crystals suitable for X-ray diffraction were grown from a saturated diethyl ether solution at −30 °C. ^{1}H NMR (300 MHz, C_7D_8): δ 26.63 (br s, 2H), 14.10 (d, 2H), 8.27 (br t, 1H), 0.68 (app t, 2H), 0.36 (app d, 2H) -1.59 (s, 14H), -2.46 (br s, 2H), -2.79 (s, 2H), -3.67 (app q, 2H), -3.90 (app d, 2H), -4.08 (m, 8H), -4.78 (app t, 2H), -6.78 (d, 2H), -7.67 (d, 2H), -8.89 (br s, 2H), -10.91 (br s, 2H), -11.58 (br s, 2H), -11.91 (br s, 2H), -13.00 (br s, 2H), -21.99 (s, 3 Me), -22.2 (br s, 2H), -24.78 (s, 2H), -36.85 (s, 2H), -38.99 (s, 2H), -41.53 (s, 2H). Anal. Calcd for $C_{45}H_{70}BFeNO_2P_2$: C, 68.79; H, 8.98; N, 1.78. Found: C, 67.28; H, 9.33; N, 1.86.

[Fe(C{Ph}C{C≡CPh}Bpin)(^{Cy}PNP)], 7a. A scintillation vial was charged with 0.102 g (0.14 mmol) of **1·py** and 5 mL of THF. While stirring, 0.040 g (0.16 mmol) of B_2pin_2 were added to the light brown solution. The mixture changed colour to deep purple after 10 minutes, then 0.16 mmol of 1,4-diphenylbutadiyne

were added. The reaction solution rapidly changed to a bright red colour, and it was allowed to continue stirring for 12 h. After this time, all volatiles were removed in vacuo and the remaining residue was extracted into toluene. The solution was then filtered through a pad of Celite, and the toluene evaporated to dryness. The remaining red solids were washed with cold pentane and isolated by filtration yielding 0.102 g (82 %) of red material. Crystals suitable for X-ray diffraction were grown from vapor diffusion of pentane into THF. ^{1}H NMR (C_6D_6): δ 30.01 (br s, 2H), 18.77 (s, 2H), 15.08 (s, 1H), 12.35 (s, 1H), 11.90 (s, 2H), -0.66 (br s, 12H), -0.90 (br s, 2H), -1.06 (d, 1H), -1.30 (d, 2H), -1.60 (br s, 2H), -2.24 (br s, 4H), -2.80 (d, 2H), -3.02 (br s, 4H), -3.21 (br s, 2H), -3.45 (br s, 1H), -4.12 (br s, 2H), -4.43 (br s, 4H), -7.13 (d, 2H), -7.89 (br s, 2H), -8.10 (d, 2H), -8.20 (br s, 4H), -8.45 (br s, 2H), -10.85 (br s, 2H), -11.70 (br s, 2H), -16.66 (br s, 2H), -29.06 (s, 2H), -35.38 (br s, 2H), -42.16 (br s, 2H), -43.97 (br s, 2H). Anal. Calcd for $C_{52}H_{72}BFeNO_2P_2$: C, 71.65; H, 8.33; N, 1.61. Found: C, 67.62; H, 8.20; N, 1.39. Low values for C are consistent with retention of excess B_2pin_2 used in the preparation.

[Fe(C{Ad}NBpin)(^{Cy}PNP)], 8. A flask was charged with 0.0704 g (0.098 mmol) of **1·py** and 5 mL of THF. To the stirring solution was added 0.0276 g (0.109 mmol) of B_2pin_2 as a solid in one portion. The mixture was allowed to stir at room temperature until it became deep dark purple in colour. Once the desired colour was observed, 0.0190 g (0.118 mmol) of 1-cyanoadamantane was added. The colour rapidly changed to bright red and the solution was allowed to stir at room temperature overnight. All volatiles were removed in vacuo and the dark red residue was extracted into toluene and then filtered through a pad of Celite. The resulting solution was evaporated to dryness affording 0.054 g (71 %) of a red solid. Crystals suitable for X-ray diffraction were grown by slow cooling of a saturated heptane solution at −30 °C. NMR (C_6D_6): ^{1}H δ 30.08 (br s, 6 Ad), 9.96 (app d, 3 Ad), 9.43 (app d, 3 Ad), 5.01 (s, 3 Ad), 3.02 (s, 12 Bpin), -1.02 (app d, 2 Cy), -1.34 (app t, 2 Cy), -1.72 (app d, 2 Cy), -3.52 (app q, 2 Cy), -3.93 (app d, 2 Cy), -4.45 (app t, 2 Cy), -5.07 (app q, 2 Cy), -5.87 (m, 4 Cy), -6.05 (m, 2 Cy), -6.81 (br s, 4 Cy), -9.03 (app d, 2 Cy), -9.23 (app d, 2 Cy), -12.69 (br s, 2 Cy), -13.79 (br s, 2H), -14.87 (app d, 4H), -16.09 (s, pyr-C*H*), -16.42 (br s, 2H), -17.43 (br s, 2H), -25.6 (br s, 2H), -33.2 (br s, 2H), -35.5 (br s, 2H), -71.6 (br s, 2H). Anal. Calcd for $C_{47}H_{77}BFeN_2O_2P_2{\cdot}C_7H_{16}$: C, 69.67; H, 10.07; N, 3.01. Found: C, 69.24; H, 9.96; N, 2.94.

Acknowledgements

The authors thank the Welch Foundation (AX-1772) for financial support of this work. NMR and X-ray facilities at UTSA were acquired with support from the National Science Foundation (CHE-1625963 and CHE-1920057).

Accession Codes

CCDC 2204986-2204994 contain the supplementary crystallographic data for this paper. These data can be obtained free of charge via www.ccdc.cam.ac.uk/data_request/cif, or by emailing data_request@ccdc.cam.ac.uk, or by contacting The Cambridge Crystallographic Data Centre, 12 Union Road, Cambridge CB2 1EZ, UK; fax: +44 1223 336033.

Author Information

Corresponding Author
*E-mail: zachary.tonzetich@utsa.edu

Author Contributions

The manuscript was written through contributions of all authors. All authors have given approval to the final version of the manuscript.

Notes and references

1. G. J. Irvine, M. J. G. Lesley, T. B. Marder, N. C. Norman, C. R. Rice, E. G. Robins, W. R. Roper, G. R. Whittell and L. J. Wright, *Chem. Rev.*, 1998, **98**, 2685-2722.
2. M. Yamashita and K. Nozaki, in *Synthesis and Application of Organoboron Compounds*, eds. E. Fernández and A. Whiting, Springer International Publishing, Cham, 2015, pp. 1-37.
3. H. Braunschweig and M. Colling, *Coord. Chem. Rev.*, 2001, **223**, 1-51.
4. U. Kaur, K. Saha, S. Gayen and S. Ghosh, *Coord. Chem. Rev.*, 2021, **446**, 214106.
5. L. Dang, Z. Lin and T. B. Marder, *Chem. Commun.*, 2009, 3987-3995.
6. S. K. Bose, L. Mao, L. Kuehn, U. Radius, J. Nekvinda, W. L. Santos, S. A. Westcott, P. G. Steel and T. B. Marder, *Chem. Rev.*, 2021, **121**, 13238-13341.
7. J. I. van der Vlugt, *Angew. Chem. Int. Ed.*, 2010, **49**, 252-255.
8. Z. Lin, in *Computational Studies in Organometallic Chemistry*, eds. S. A. Macgregor and O. Eisenstein, Springer International Publishing, Cham, 2016, pp. 39-58.
9. S. Aldridge and D. L. Coombs, *Coord. Chem. Rev.*, 2004, **248**, 535-559.
10. H. Braunschweig, R. D. Dewhurst and A. Schneider, *Chem. Rev.*, 2010, **110**, 3924-3957.
11. A. A. Dickinson, D. J. Willock, R. J. Calder and S. Aldridge, *Organometallics*, 2002, **21**, 1146-1157.
12. X. Guo, T. Yang, F. K. Sheong and Z. Lin, *ACS Catal.*, 2021, **11**, 5061-5068.
13. T. R. Cundari and Y. Zhao, *Inorg. Chim. Acta*, 2003, **345**, 70-80.
14. H. Braunschweig, *Angew. Chem. Int. Ed.*, 1998, **37**, 1786-1801.
15. D. L. Kays and S. Aldridge, in *Contemporary Metal Boron Chemistry I: Borylenes, Boryls, Borane σ-Complexes, and Borohydrides*, eds. T. B. Marder and Z. Lin, Springer Berlin Heidelberg, Berlin, Heidelberg, 2008, pp. 29-122.
16. T. J. Mazzacano and N. P. Mankad, *Chem. Commun.*, 2015, **51**, 5379-5382.
17. F. Rami, F. Bächtle and B. Plietker, *Catal. Sci. Technol.*, 2020, **10**, 1492-1497.
18. A. J. MacNair, C. R. P. Millet, G. S. Nichol, A. Ironmonger and S. P. Thomas, *ACS Catal.*, 2016, **6**, 7217-7221.
19. L. Britton, J. H. Docherty, A. P. Dominey and S. P. Thomas, *Molecules*, 2020, **25**.
20. J. Y. Wu, B. Moreau and T. Ritter, *J. Am. Chem. Soc.*, 2009, **131**, 12915-12917.

21. M. Haberberger and S. Enthaler, *Chem. Asian. J.*, 2013, **8**, 50-54.
22. C. Wang, C. Wu and S. Ge, *ACS Catal.*, 2016, **6**, 7585-7589.
23. L. Zhang, D. Peng, X. Leng and Z. Huang, *Angew. Chem. Int. Ed.*, 2013, **52**, 3676-3680.
24. M. Kamitani, H. Kusaka and H. Yuge, *Chem. Lett.*, 2019, **48**, 898-901.
25. T. Dombray, C. G. Werncke, S. Jiang, M. Grellier, L. Vendier, S. Bontemps, J.-B. Sortais, S. Sabo-Etienne and C. Darcel, *J. Am. Chem. Soc.*, 2015, **137**, 4062-4065.
26. R. B. Bedford, P. B. Brenner, E. Carter, T. Gallagher, D. M. Murphy and D. R. Pye, *Organometallics*, 2014, **33**, 5940-5943.
27. T. Kato, S. Kuriyama, K. Nakajima and Y. Nishibayashi, *Chem. Asian. J.*, 2019, **14**, 2097-2101.
28. K. Nakajima, T. Kato and Y. Nishibayashi, *Org. Lett.*, 2017, **19**, 4323-4326.
29. T. C. Atack, R. M. Lecker and S. P. Cook, *J. Am. Chem. Soc.*, 2014, **136**, 9521-9523.
30. W. Su, R.-X. Qiao, Y.-Y. Jiang, X.-L. Zhen, X. Tian, J.-R. Han, S.-M. Fan, Q. Cheng and S. Liu, *ACS Catal.*, 2020, **10**, 11963-11970.
31. A. L. Narro, H. D. Arman and Z. J. Tonzetich, *Inorg. Chem.*, 2022, **61**, 10477-10485.
32. B. L. Tran, D. Adhikari, H. Fan, M. Pink and D. J. Mindiola, *Dalton Trans.*, 2010, **39**, 358-360.
33. C. V. Thompson, H. D. Arman and Z. J. Tonzetich, *Organometallics*, 2022, **41**, 430-440.
34. H. Braunschweig, K. Radacki, F. Seeler and G. R. Whittell, *Organometallics*, 2004, **23**, 4178-4180.
35. C. V. Thompson, H. D. Arman and Z. J. Tonzetich, *Organometallics*, 2017, **36**, 1795-1802.
36. C. V. Thompson, I. Davis, J. A. DeGayner, H. D. Arman and Z. J. Tonzetich, *Organometallics*, 2017, **36**, 4928-4935.
37. N. Paul, T. Patra and D. Maiti, *Asian. J. Org. Chem.*, 2022, **11**, e202100591.
38. M. A. Esteruelas, M. Oliván and A. Vélez, *J. Am. Chem. Soc.*, 2015, **137**, 12321-12329.
39. S. Moorhouse and G. Wilkinson, *J. Organomet. Chem.*, 1976, **105**, 349-355.
40. S. Garhwal, N. Fridman and G. de Ruiter, *Inorg. Chem.*, 2020, **59**, 13817-13821.
41. S. Mandal, S. Mandal and K. Geetharani, *Chem. Asian. J.*, 2019, **14**, 4553-4556.
42. G. Vijaykumar, M. Bhunia and S. K. Mandal, *Dalton Trans.*, 2019, **48**, 5779-5784.
43. X. Sun, P. Gu, J. Qin and Y. Su, *Chem. Commun.*, 2020, **56**, 12379-12382.
44. A. M. Poitras, L. K. Oliemuller, G. P. Hatzis and C. M. Thomas, *Organometallics*, 2021, **40**, 1025-1031.
45. S. Jiang, S. Quintero-Duque, T. Roisnel, V. Dorcet, M. Grellier, S. Sabo-Etienne, C. Darcel and J.-B. Sortais, *Dalton Trans.*, 2016, **45**, 11101-11108.
46. *CrysAlisPro*, Rigaku Oxford Diffraction: Rigaku Corporation, The Woodlands, TX, 2015.
47. *SCALE3 ABSPACK -An Oxford Diffraction program*, Oxford Diffraction Ltd.: 2005.
48. O. V. Dolomanov, L. J. Bourhis, R. J. Gildea, J. A. K. Howard and H. Puschmann, *J. Appl. Crystallogr.*, 2009, **42**, 339-341.
49. G. Sheldrick, *Acta Crystallogr., Sect. A*, 2015, **71**, 3-8.
50. G. M. Sheldrick, *Acta Crystallogr., Sect. A*, 2008, **A64**, 112-122.